Title

Restoring Ureagenesis in Hepatocytes by CRISPR/Cas9-mediated Genomic Addition to Arginase-deficient Induced Pluripotent Stem Cells.

Journal

Molecular therapy. Nucleic acids, 5(11)

ISSN

2162-2531

Authors

Lee, Patrick C
Truong, Brian
Vega-Crespo, Agustin
et al.

Publication Date

2016-11-01

DOI

10.1038/mtna.2016.98

Peer reviewed

Citation: Molecular Therapy—Nucleic Acids (2016) 5, e394; doi:10.1038/mtna.2016.98
Official journal of the American Society of Gene & Cell Therapy

www.nature.com/mtna

Restoring Ureagenesis in Hepatocytes by CRISPR/Cas9-mediated Genomic Addition to Arginase-deficient Induced Pluripotent Stem Cells

Patrick C Lee[1,2], Brian Truong[1,2], Agustin Vega-Crespo[1,2], W Blake Gilmore[3], Kip Hermann[1,3], Stephanie AK Angarita[3], Jonathan K Tang[1,2], Katherine M Chang[1,2], Austin E Wininger[3], Alex K Lam[3], Benjamen E Schoenberg[1,2], Stephen D Cederbaum[4–6], April D Pyle[7], James A Byrne[1,2] and Gerald S Lipshutz[1–6,8,9]

Urea cycle disorders are incurable enzymopathies that affect nitrogen metabolism and typically lead to hyperammonemia. Arginase deficiency results from a mutation in *Arg1,* the enzyme regulating the final step of ureagenesis and typically results in developmental disabilities, seizures, spastic diplegia, and sometimes death. Current medical treatments for urea cycle disorders are only marginally effective, and for proximal disorders, liver transplantation is effective but limited by graft availability. Advances in human induced pluripotent stem cell research has allowed for the genetic modification of stem cells for potential cellular replacement therapies. In this study, we demonstrate a universally-applicable CRISPR/Cas9-based strategy utilizing exon 1 of the hypoxanthine-guanine phosphoribosyltransferase locus to genetically modify and restore arginase activity, and thus ureagenesis, in genetically distinct patient-specific human induced pluripotent stem cells and hepatocyte-like derivatives. Successful strategies restoring gene function in patient-specific human induced pluripotent stem cells may advance applications of genetically modified cell therapy to treat urea cycle and other inborn errors of metabolism.

Molecular Therapy—Nucleic Acids (2016) **5**, e394; doi:10.1038/mtna.2016.98; published online 29 November 2016
Subject Category: gene addition deletion and modification therapeutic proof of concept

Introduction

Urea cycle disorders (UCDs) are rare enzymopathies with an incidence of 1:35,000 births resulting in ~113 new cases per year in the United States.[1] They are a significant cause of inherited hyperammonemia and afflicted infants, while newborns are at substantial risk of recurrent brain injury and death. Excessive plasma ammonia is neurotoxic, resulting in central nervous system injury including intellectual disabilities, seizures, and loss of psychomotor function[1–5]; they also live with continued nitrogen vulnerability. UCDs result from a deficiency in one of six hepatic enzymes or two mitochondrial transporters that regulate nitrogen metabolism and urea production[1–3,5] which are typically classified as an inborn errors of metabolism.

Hyperargininemia, or arginase deficiency, is an autosomal recessive disorder that affects the final step of the urea cycle. Patients who exhibit hyperargininemia typically present, after the neonatal period, with spasticity, seizures, spastic diplegia, and developmental regression, differing from the other UCDs.[5–8] Arginase 1 (*Arg1*) is primarily located in the liver, hydrolyzing arginine to urea while regenerating ornithine to continue the cycle.[6,8] Loss of *Arg1* activity results in an inability to remove nitrogen from arginine, but rarely causes symptoms of hyperammonemia. Instead, the cause of the pathogenesis of neurological deterioration in arginase deficiency is not known and is thought to be due to unique biochemical abnormalities such as elevated guanidino compounds, nitric oxide, or glutamine.[3,8–10]

As there is no completely effective treatment for UCDs, the mainstay of therapy is dietary protein restriction, with emergency treatments for hyperammonemia consisting of dialysis, hemofiltration, and administration of nitrogen scavenging drugs.[5] Chronic therapy is minimally effective in reducing plasma ammonia while control of hyperargininemia may delay the onset of symptoms[6,8] but may not ultimately prevent the progressive and relentless nature of neurocognitive decline. Liver transplantation is the extreme alternative to conventional therapies to prevent progression of neurological injury in UCD patients. However, the demand for liver donors far exceeds the supply, and other avenues, such as genetic modification and cell replacement therapy, need to be explored to treat these disorders.

Since the demonstration that human induced pluripotent stem cells (hiPSCs) could be reprogrammed from fibroblasts with four transcription factors (*Oct4*, *Sox2*, *Klf4*, and *cMyc*), hiPSCs have emerged as a potential avenue for patient-specific disease modeling and development of therapy.[11–15]

The first two authors contributed equally to this work.

[1]Department of Molecular and Medical Pharmacology, David Geffen School of Medicine at UCLA, Los Angeles, California, USA; [2]Eli and Edythe Broad Center of Regenerative Medicine and Stem Cell Research, David Geffen School of Medicine at UCLA, Los Angeles, California, USA; [3]Department of Surgery, David Geffen School of Medicine at UCLA, Los Angeles, California, USA; [4]Department of Psychiatry, David Geffen School of Medicine at UCLA, Los Angeles, California, USA; [5]Intellectual and Developmental Disabilities Research Center at UCLA, Los Angeles, California, USA; [6]Semel Institute for Neuroscience, UCLA, Los Angeles, California, USA; [7]Department of Microbiology, Immunology and Molecular Genetics, UCLA, David Geffen School of Medicine at UCLA, Los Angeles, California, USA; [8]Department of Medicine, David Geffen School of Medicine at UCLA, Los Angeles, California, USA; [9]Department of Urology, David Geffen School of Medicine at UCLA, Los Angeles, California, USA. Correspondence: Gerald S. Lipshutz, 77–120 Center for the Health Sciences, David Geffen School of Medicine at UCLA, Los Angeles, California 90095–7054, USA. E-mail: glipshutz@mednet.ucla.edu

Keywords: arginase; genomic addition; hepatocytes; PSCs; urea cycle
Received 14 June 2016; accepted 26 September 2016; advance online publication 29 November 2016. doi:10.1038/mtna.2016.98

Whereas the difficulty in obtaining primary cell cultures previously hindered progress of disease research, the ability of patient-specific hiPSCs to differentiate into genetically similar somatic cell types of various lineages, such as hepatocytes, allows for the generation of a substantial quantity of patient-specific cells.[16,17] These hiPSC-derived hepatocytes express liver-specific markers such as albumin (*ALB*), alpha-fetoprotein (*AFP*), and cytokeratin 18 (*CK18*) as well as functionality markers such α1-antitrypsin (*AAT*) and *CYP3A4*, demonstrating their phenotypic similarity to endogenously derived hepatocytes.[17] Reprogramming patient-specific hiPSCs and establishing isogenic and functional derivatives afford the advantage of avoiding the ethical controversy of oocyte-derived embryonic stem cell use and potentially addressing the immunogenicity issues for cell replacement therapies.[18]

In this study, we sought to correct the enzyme deficiency, using a universal approach, in multiple arginase-deficient hiPSC lines derived from hyperargininemic patients by using genome editing technology. We delivered clustered interspaced short palindromic repeats (CRISPR)/Cas9 nickases via nucleofection for gene addition of a full-length codon-optimized human arginase 1 cDNA (ArgO) expression cassette (**L**eft homologous arm-h**E**F1a-**A**rgO-IRES-**P**uro(R)-**R**ight homologous arm (LEAPR)) into Exon 1 of the endogenous hypoxanthine-guanine phosphoribosyltransferase (HPRT) locus in hiPSCs.[19] After targeted insertion and puromycin selection (enabled by the LEAPR-derived puromycin N-acetyltransferase (PAC)), and with confirmation of the presence of the LEAPR cassette in the patient-specific hiPSCs, we demonstrated the restoration of arginase activity in both hiPSCs and differentiated hepatocyte-like cells. Results from this genetic targeting approach potentially offer a widely applicable method to genetically introduce arginase expression in hiPSCs derived from hyperargininemic patients and, on a broader scale, to other single-enzyme inborn errors of metabolism.

Results

Derivation of patient-specific hiPSCs from arginase-deficient dermal fibroblasts

We derived genetically-distinct hiPSC lines from dermal fibroblasts taken from three patients with hyperargininemia. The first disease dermal fibroblast line, AD1, originating from a female argininemic patient, was purchased from Coriell (GM00954). Two additional dermal fibroblast lines, AD2 and AD3, were derived from skin punch biopsies obtained from a male and female patient, respectively. The AD dermal fibroblasts were successfully reprogrammed to hiPSCs using a lentiviral vector expressing a constitutive polycistronic cassette (STEMCCA) encoding the four transcription factors *OCT4*, *SOX2*, *KLF4*, and *cMyc*.[11,20,21] Dermal fibroblasts were transduced with the STEMCCA lentivirus and were maintained in culture for 30 days on mouse embryonic fibroblasts before conversion to feeder-free culture conditions. The control hiPSC line (xc-HUF1), derived from the dermal fibroblasts of a healthy adult male was previously established in the lab using the same reprogramming methodology.[22]

AD1, AD2, and AD3 hiPSC lines exhibited normal stem cell-like morphology throughout the course of the study. Characterization of the AD hiPSCs included immunophenotyping for common pluripotent stem cell markers, alkaline phosphatase staining, *in vivo* teratoma formation, and karyotype analysis. AD1, AD2, and AD3 hiPSCs stained positive for pluripotency markers: Oct4, NANOG, SSEA-3, SSEA-4, Tra-1–60, Tra-1–81 and all exhibited positive alkaline phosphatase activity (**Figure 1a**). Normal karyotypic analyses, with no genomic abnormalities, were detected through G-banding studies of AD1, AD2, and AD3 hiPSC lines (**Figure 1b**). Furthermore, AD hiPSCs were collected and injected subcutaneously into the hindleg of SCID mice for *in vivo* teratoma analysis. Teratoma sections from AD1, AD2, and AD3 were stained with H&E and exhibited formation of gut (endoderm), neuroectoderm (ectoderm), and chondrocyte (mesoderm) derivatives, demonstrating the ability of our hiPSCs to form tissues from all three germ layers (**Figure 1c**). Additionally, the specific arginase mutations were determined for each line (**Figure 1d**). Characterization of all three diseased hiPSCs was compared with nondiseased controls as xc-HUF1 hiPSCs and demonstrated no difference in pluripotency profile (data not shown).

Design of ArgO and vectors for gene correction of hiPSCs

To correct for the mutant *Arg1* gene in our patient-derived AD hiPSCs, we designed a selectable, full-length codon-optimized human arginase cDNA (ArgO) expression cassette under the constitutive control of the human elongation factor 1α (hEF1α) promoter, referred to as LEAPR, to be inserted into Exon 1 of the HPRT locus (**Figure 2a**). Utilizing CRISPR/Cas9 nickases to bind and cleave Exon 1 of HPRT, we achieved targeted LEAPR addition into this desired site. LEAPR addition and disruption of the HPRT locus allowed for secondary positive clonal selection of successful on-target integration via resistance to 6-thioguanine (6-TG) treatment. Additionally, a puromycin resistance gene encoded within the LEAPR construct afforded the ability to utilize an efficient dual selection method to isolate a clonal population of cells that successfully integrated our vector into the HPRT locus. After dual selection with puromycin and 6-TG, AD1, AD2, and AD3 hiPSCs maintained normal stem cell-like morphology (data not shown).

Evaluation of targeted integration and expression of ArgO into corrected hiPSCs

After delivery of the LEAPR construct, we performed experiments to verify correct on-target integration into the AD hiPSCs. AD hiPSCs were first dual-selected by two cycles of 1 μg/ml puromycin treatment for 72 hours followed by 6-TG treatment. Dual-resistant cell populations were then clonally selected into three subclones each for all AD hiPSC lines. To analyze the targeted integration of our donor vector into Exon 1 of the HPRT locus, primers were designed to span each junction between the endogenous genome and our inserted vector. For each junction, one primer was designed to bind a region of the genome outside of the homologous arm region, and another was designed to bind a sequence within our inserted donor vector. Products at both 5′ and 3′ junction sites demonstrated on-target integration of our LEAPR construct in each of three subclones of the corrected AD1, AD2, and AD3 hiPSC lines (**Figure 2b** (for AD1) and

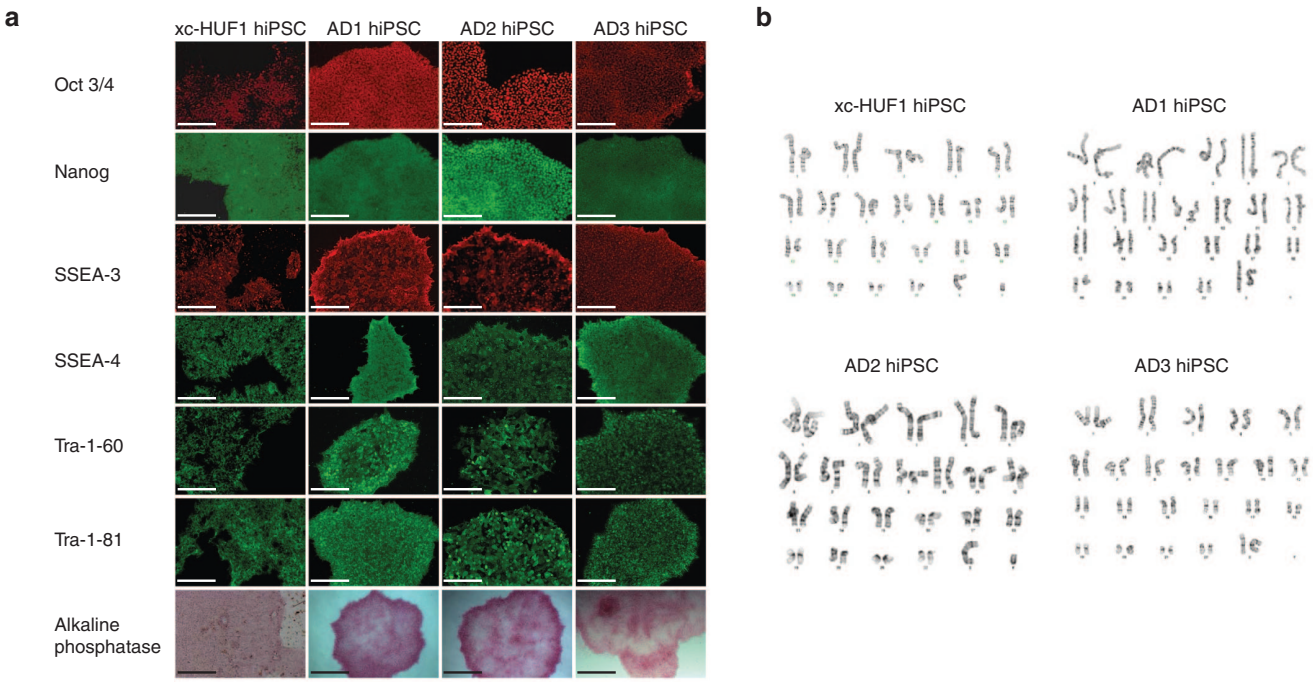

d

Line	Source	Mutation	Notes
AD1	Coriell GM00954	1. c.892 G>C p.Ala298Pro (A298P) 2. c.61 C>T p.Arg21Ter (R21X)	Female, Hispanic, 4 years old 1. Heterozygous, disease causing 2. Heterozygous, disease causing
AD2	UCLA	1. c.61 C>T p.Arg21Ter(R21X) 2. c.709 G>A p.Asp237Asn (D237N)	Male, Asian, 23 years old 1. Heterozygous, disease causing 2. Heterozygous, disease causing
AD3	UCLA	1. c.365 G>A p.Trp122Ter (W122X)	Female, Hispanic, 52 years old 1. Homozygous, disease causing

Figure 1 Characterization of arginase deficient (AD) human induced pluripotent stem cells (hiPSCs). (**a**) Pluripotency of all three AD hiPSC lines was measured via immunophenotyping. AD1, AD2, and AD3 subclones were positive for octamer-binding transcription factor-4 (OCT3/4), homeobox protein nanog (NANOG), stage-specific embryonic antigens 3 (SSEA-3) and 4 (SSEA-4), tumor-related antigens 1–60 (TRA-1–60) and 1–81 (TRA-1–81), and alkaline phosphatase. AD hiPSCs were compared with a wild type hiPSC line xc-HUF1. (Scale bars for all images are 200 μm except alkaline phosphatase which is 500 μm.) (**b**) AD1, AD2, and AD3 hiPSC lines exhibited normal 46 XX or 46 XY karyotypes, and (**c**) demonstrated the ability to form tissues from all three germ layers: gut (endoderm), chondrocytes (mesoderm), and neuroectoderm (ectoderm). (Scale bars = 200 μm) (**d**) Sequencing analysis reveals specific arginase mutations in each line.

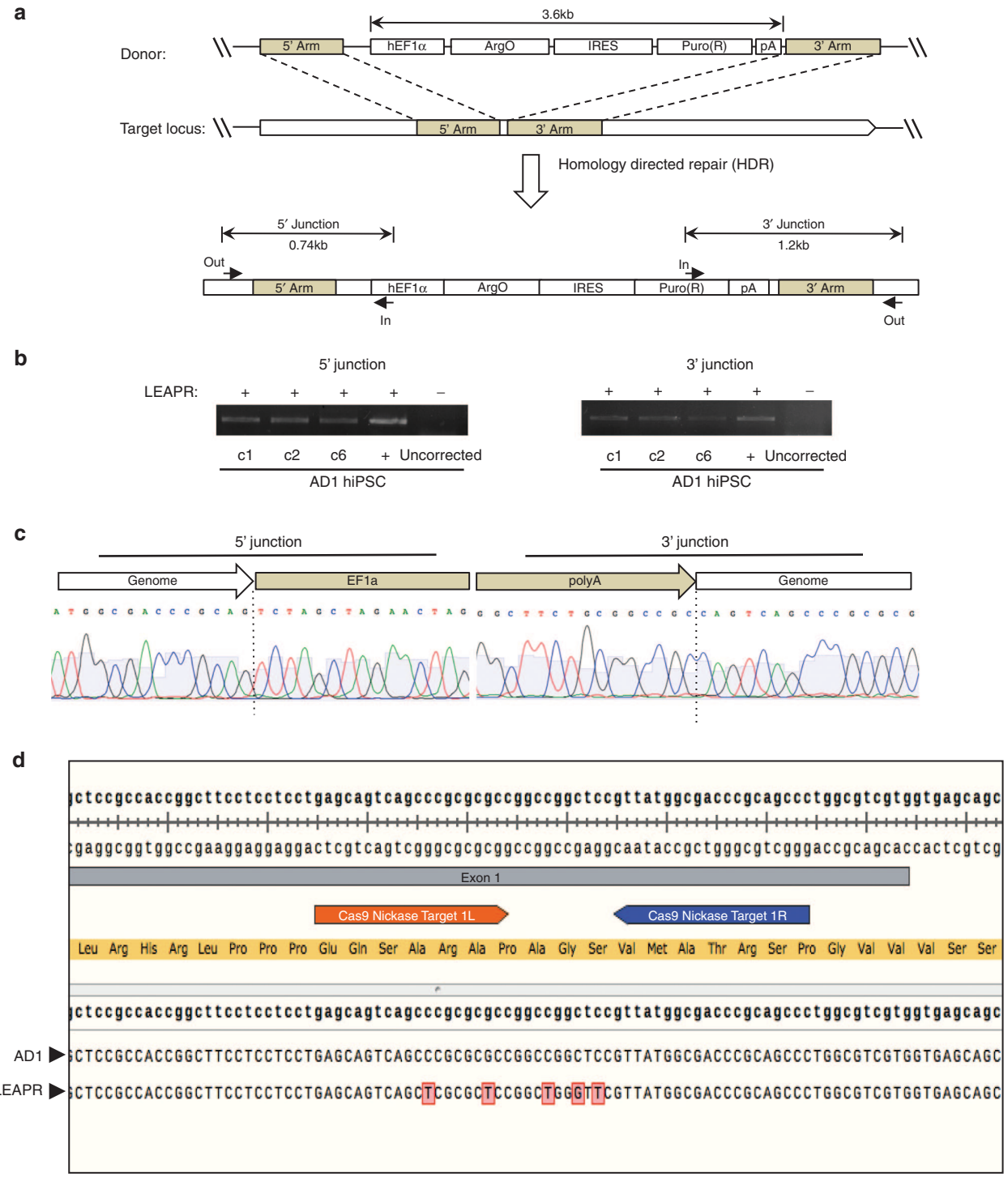

Figure 2 Design and integration of LEAPR expression cassette. (**a**) Design of the LEAPR construct containing the human codon optimized arginase (*ArgO*). (**b**) Junction PCR was performed to determine integration of the construct in both wild-type xc-HUF1 and AD1 hiPSCs in Exon 1 of the HPRT site. (**c**) Sequencing analysis was performed on the integration of the construct in AD1 hiPSCs at the target site (See also **Supplementary Figure S1**). (**d**) Genomic integration of LEAPR into the HPRT locus (located on X chromosome) was determined for AD1 (female, XX, *i.e.*, two HPRT alleles) by site-specific sequencing at the nuclease target sites (see also **Supplementary Figure S2**). While sequencing confirmed that the other allele of HPRT was not integrated with the donor construct, nuclease activity introduced five genetic mutations (noted by red boxes); the fifth resulted in a serine to phenylalanine amino acid change (TCC →TTC). AD, arginase deficient; hiPSCs, human induced pluripotent stem cells; HPRT, hypoxanthine-guanine phosphoribosyltransferase; LEAPR, **L**eft homologous arm-h**E**F1a-**A**rgO-IRES-**P**uro(R)-**R**ight homologous arm; PCR, polymerase chain reaction.

Supplementary Figure S1 (for AD2 and AD3)). Additionally, sequencing analysis of the junction PCR products showed the seamless transition between donor vector sequence and the endogenous genome sequence of our gene-corrected cell lines at both the 5′ and 3′ junctions of our gene cassette insert (**Figure 2c** (for AD1) and **Supplementary Figure S1** (for AD2 and AD3)).

To further characterize the targeted integration of LEAPR into the AD hiPSCs, we utilized quantitative reverse transcription-polymerase chain reaction (qRT-PCR) to determine whether the LEAPR construct integrated into one or both HPRT alleles in corrected AD1 and AD3 LEAPR hiPSCs and also used sequencing technology to further examine AD1. As AD1 and AD3 are XX and AD2 is XY, qRT-PCR confirmed and demonstrated twice the levels of genomic HPRT (gHPRT) in AD1 and AD3 compared with AD2 relative to genomic glyceraldehyde 3-phosphate dehydrogenase (gGAPDH) (**Supplementary Figure S2**, top). Furthermore, qRT-PCR demonstrated equal amplification of ArgO, a unique element of the LEAPR construct, relative to gGAPDH demonstrating an equal number of LEAPR integrations throughout the genomes of AD LEAPR hiPSCs (**Supplementary Figure S2**, middle). Finally, qRT-PCR demonstrated AD1 and AD3 with half the level of ArgO compared with AD2, relative to HPRT consistent with the integration of 1 LEAPR copy per two HPRT alleles in AD1 and AD3 and one LEAPR copy per one HPRT allele in AD2 (**Supplementary Figure S2**, bottom). We also sequenced the other HPRT allele of AD1 which showed lack of integration, confirming that only one allele had the integrated donor arginase construct. However, because of nuclease activity at that site, five genetic mutations were introduced in the other HPRT allele, the first four being silent mutations and the fifth resulting in a serine to phenylalanine amino acid change (**Figure 2d**).

Off-target analysis was performed in AD1 LEAPR hiPSCs to determine and quantify potential insertions and deletions due to off-target sequence homology for nickases A and B. High probability sites for off-target nickase binding for each nuclease were determined *in silico* (probability scores of 1.37, 0.86, and 0.86 for nickase A and 0.58 for nickase B (out of a maximum score of 100)) were examined via sequencing. Analysis demonstrated 0% insertions and deletions at all sites (**Supplementary Figure S3a,b**).

Arginase levels were examined in the LEAPR-corrected hiPSC lines by measuring RNA expression via qRT-PCR and functionality via urea production (*i.e.*, restoring ureagenesis). After puromycin and 6-TG selection, corrected hiPSCs (n = 3) expressed significantly higher RNA levels ($P < 0.0001$) of codon optimized arginase compared with wild type arginase RNA levels in uncorrected AD hiPSCs, demonstrating on-target integration and expression in all three corrected hiPSC lines. The integration of *ArgO* increased arginase mRNA levels in AD1, AD2, and AD3 hiPSCs to 57, 92, and 46% (replicates of n = 3 per sample) respectively when compared with wild type arginase levels in human fetal liver (**Figure 3a** (for AD1) and **Supplementary Figure S4** (for AD2 and AD3)). Additionally, all corrected AD hiPSCs exhibited a significant increase ($P < 0.0001$) in urea production itself (*i.e.*, functional activity) when compared with their uncorrected counterparts. Functionality of corrected AD1 hiPSCs increased to 102% (P = 0.0212) of that measured in human fetal liver levels (**Figure 3b** for AD1). Varying degrees of recovery were observed in AD1, AD2, and AD3 corrected lines; however, the lowest recorded recovery level was still 71% of the primary fetal liver (**Figure 3b** and **Supplementary Figure S5** for AD2 and AD3). Taken together, these data demonstrate (i) a high specificity of integration into Exon 1 of the *HPRT* target site as well as (ii) a high codon optimized arginase RNA expression with substantial functional arginase enzyme activity in hiPSCs.

Directed differentiation of human pluripotent cells into hepatocyte-like cells

Using a previously published protocol,[17] we differentiated the corrected AD1, AD2, and AD3 hiPSCs, their uncorrected

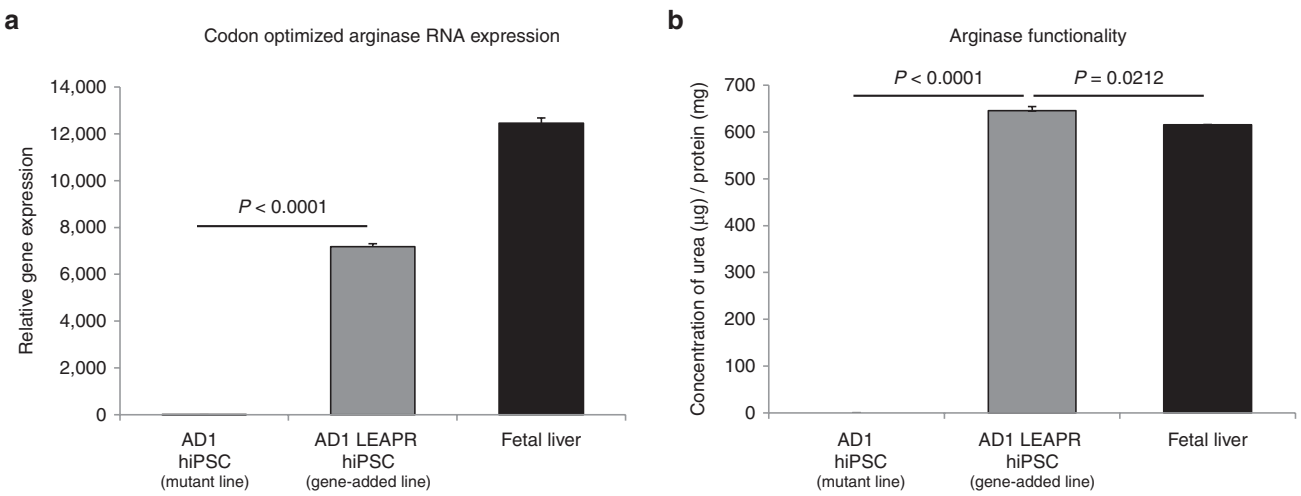

Figure 3 Measuring *ArgO* in AD hiPSCs. (**a**) Relative gene expression of *ArgO*, measured against glyceraldehyde 3-phosphate dehydrogenase (GAPDH), in AD1 uncorrected and corrected hiPSCs was measured by quantitative reverse transcription-polymerase chain reaction (qRT-PCR) in technical triplicate (n = 3). (**b**) After integration of *ArgO* in AD1 hiPSCs urea production was measured and compared with fetal liver (n = 2). Functionality experiments were performed in technical duplicate. (Data are represented as mean ± SD.) AD, arginase deficient; *ArgO*, codon optimized arginase; hiPSCs, human induced pluripotent stem cells; SD, standard deviation.

counterparts, and control xc-HUF1 hiPSCs into hepatocyte-like cells. After 21 days, we assessed expression of specific liver markers and assessed liver cell-specific functions of our derivatives. Morphology of the genetically modified AD1 LEAPR hepatocyte-like cells resembled both that of their uncorrected counterparts (AD1 hepatocytes) and primary human adult hepatocytes (shown in **Figure 4a**; AD2 and AD3 shown in **Supplementary Figure S6a**).

At the end of the final differentiation stage, we characterized the expression of hepatic markers in our derivatives. Similar to the primary adult hepatocyte control, LEAPR-corrected AD1, AD2, and AD3 derivatives stained positive for albumin (**Figure 4a** for AD1 and **Supplementary Figure S6a** for AD2 and AD3 respectively). The hepatocyte-like cells exhibited expression of *AFP*, whereas the primary adult hepatocyte control was essentially negative for *AFP* (**Figure 4a**). This

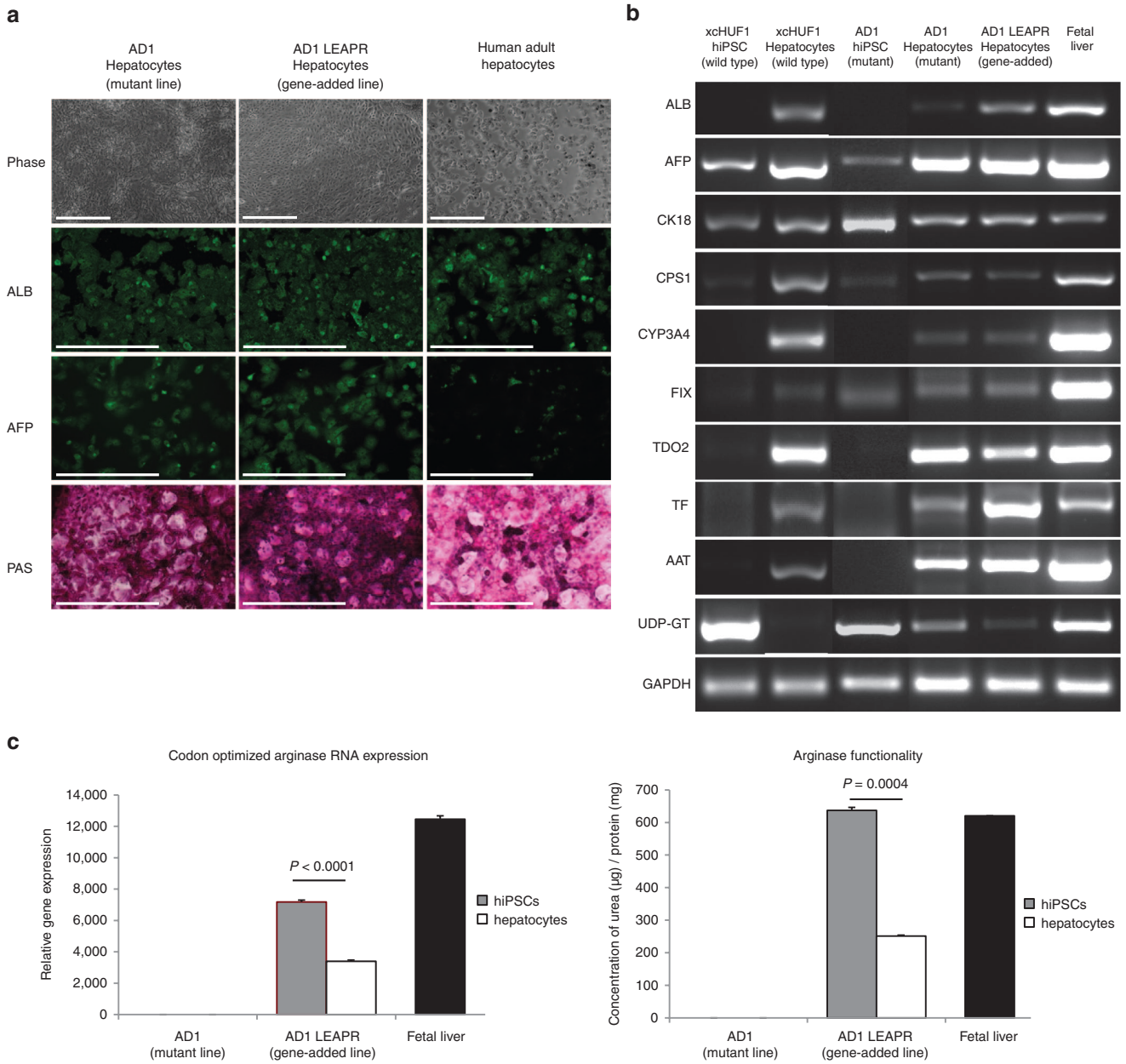

Figure 4 Characterization of hepatocyte-like cells. (**a**) Derived uncorrected and corrected (gene added) AD1 hepatocyte-like were examined and morphology compared with primary adult hepatocytes *in-vitro* (Scale bars = 500 µm). (**b**) Hepatic markers were examined via RT-PCR in uncorrected and corrected AD1 hepatocyte-like cells: alpha 1-antitrypsin (*AAT*), *AFP*, human serum albumin (*ALB*), cytokeratin 18 (CK18), carbamoyl phosphate synthase 1 (*CPS1*), cytochrome p450 3A4 (*CYP3A4*), factor IX (*FIX*), transferrin (*TF*), tryptophan 2,3-dioxygenase (*TDO2*), and uridine diphosphate glucuronyltransferase (*UDP-GT*). (**c**) mRNA levels of *ArgO* in hepatocyte-like cells (left panel) was compared with both unmodified and modified AD hiPSCs ($n = 3$) and unmodified hepatocyte-like cells ($n = 3$). Urea production of corrected hepatocyte-like cells (right panel) was also examined. (See also **Supplementary Figures S6ab**, **S4**, **S5**) (Data are represented as mean ± SD.) AD, arginase deficient; *ArgO*, codon optimized arginase; hiPSCs, human induced pluripotent stem cells; RT-PCR, reverse transcription polymerase chain reaction; SD, standard deviation.

observation is consistent with previous studies demonstrating that PSC-derived hepatocyte-like cells more closely mimic fetal as opposed to adult hepatocytes[23]; that is, mature hepatocytes lose *AFP* expression while more fetal-like hepatocytes continue to express *AFP*. Therefore, we compared RNA expression of multiple hepatic-specific markers of the derivatives to a human fetal liver control. RT-PCR analysis showed that AD1, AD2, and AD3 hepatocyte-like cells all expressed hepatic functional genes including: *ALB*, *AFP*, *AAT*, *CK18*, *CPS1*, *CYP3A4*, *FIX*, *TF*, *TDO2*, and *UDP-GT* (**Figure 4b** for AD1 and **Supplementary Figure S6b** for AD2 and AD3). Human primary adult hepatocytes and fetal liver were used as positive controls for the immunostaining and RT-PCR analysis, respectively.

Additionally, we assessed liver-specific functionality of both our genetically modified and unmodified AD1, AD2, and AD3 hepatocyte-like cells. At day 21, we measured glycogen storage via Periodic Acid-Schiff (PAS) staining of all hepatic derivatives. Similar to primary adult hepatocytes, corrected AD1, AD2, and AD3 hepatocyte-like cells stained positive by PAS (**Figure 4a** for AD1 and **Supplementary Figure S6a** for AD2 and AD3 respectively). These results demonstrate that genetic modification of hiPSCs with our LEAPR construct does not interfere with the capability of the cells to differentiate into hepatocyte-like cells.

Evaluation of arginase expression and functionality in hepatocyte-like cells

We examined codon optimized arginase RNA expression and functionality in the hiPSC-derived hepatocyte-like cells to determine the maintenance of arginase expression after directed differentiation. After the final differentiation step, RNA was collected from LEAPR-corrected AD1, AD2, and AD3 hepatocyte-like cells; arginase levels were quantified and compared with both corrected hiPSC and fetal liver levels via qRT-PCR. Hepatic differentiation did result in a decrease in arginase RNA expression in all three LEAPR-corrected hepatocyte-like cell lines compared with undifferentiated hiPSCs ($P < 0.0001$ for AD1; $P < 0.0002$ for AD2 and AD3) (**Figure 4c** left panel for AD1 and **Supplementary Figure S5** for AD2 and AD3 respectively). However, despite the decline in RNA expression compared with hiPSCs, AD1, AD2, and AD3 hepatocyte-like cells maintained arginase levels of 27, 39, and 36% of fetal liver *Arg1* levels (AD1, AD2, and AD3 respectively).

Next, we determined if targeted integration of the LEAPR construct affected expression of the wild type mutated arginase and other endogenous urea cycle-specific genes in the hepatocyte-like cells, specifically, carbamoyl phosphate synthase 1 (*CPS1*), which catalyzes the synthesis of carbamoyl phosphate from glutamine. We measured mRNA levels of *CPS1* in both uncorrected and corrected hiPSCs and hepatocyte-like cells (**Supplementary Figure S7**). Similar to wild type mutated arginase mRNA expression, *CPS1* levels were significantly increased postdifferentiation in both uncorrected and corrected lines ($P = 0.01$ for AD1 uncorrected lines; $P < 0.0001$ for AD1 corrected, AD2 uncorrected and corrected, and AD3 uncorrected and corrected lines). These data suggest that the increasing arginase expression with our LEAPR construct in the disease lines does not negatively impact the expression of other endogenous urea cycle-specific genes.

With the described decline in RNA expression, there was an expected postdifferentiation decline observed in ureagenesis of the LEAPR derivatives ($P = 0.0004$ for AD1; $P < 0.001$ for AD2; $P < 0.0007$ for AD3 compared with corrected hiPSCs). Importantly, though, all three corrected hepatocyte-like cell lines maintained >40% of the level of urea production (*i.e.*, arginase activity) of fetal liver (**Figure 4c**, right panel for AD1 and **Supplementary Figure S5** for AD2 and AD3 respectively).

Discussion

Chronic therapy for UCDs includes dietary restriction to limit nitrogen intake and pharmacological intervention with nitrogen scavenging drugs (*e.g.*, phenylbutyrate). Such substrate restriction is commonly used for treating UCDs while it is somewhat effective, this is more prophylactic than curative and patients remain at risk for developing long-term neurological issues due to intermittent hyperammonemia. Gene and stem cell therapy have emerged as promising therapeutic avenues to treat these disorders and prevent the development of hyperammonemia-induced neurological injury.[24–28]

Stem cells, specifically hiPSCs, provide an almost inexhaustible source of patient-specific cells that can undergo directed differentiation into various somatic cell types to be used for cellular replacement therapies.[29–31] Due to their therapeutic potential, considerable effort has been aimed into optimizing protocols to genetically modify these cells in order to model diseases and to use in potential cellular therapies.[32] However, despite the promise of utilizing genetically modified hiPSCs for therapeutic studies, the ability to efficiently deliver genes to targeted sites in hiPSCs is hampered by several challenges. Nonviral methods, such as chemical transfection or electroporation, and viral methods, via lentiviruses or adeno-associated viruses, all suffer from relatively low transfection and transduction efficiencies, transient expression, and off-target integration in the host hiPSC genome.[25,32] Recently, the development of highly specific CRISPRs and CRISPR-associated (Cas) systems to introduce genes into hiPSCs have begun to address many previous issues surrounding genomic editing of stem cells. Unlike its predecessors, such as zinc finger nucleases and transcription activator-like effector nucleases, CRISPR/Cas9 systems can be produced rapidly and introduced into specific target sites with increased accuracy.[19,33,34] As such, recent studies have demonstrated highly efficient genetic correction of hiPSCs utilizing CRISPR/Cas9 for neural and muscular disorders.[35]

The goal of this study was to determine if integration of codon-optimized arginase into three genetically distinct patient-specific hiPSCs could produce *in vitro* enzyme function after differentiation into hepatocyte-like derivatives for potential use in cellular therapy for these patients. Previous gene therapy studies have demonstrated successful reversal of disease manifestations through either treatment of neonatal mice with a helper-dependent adenoviral vector[24] or with adeno-associated virus-expressing arginase.[36] In the former, the transient nature of expression led to loss of arginase

function while in the later, long-term survival without neuropathology was achieved; however, with the loss of episomal adeno-associated virus genomes, the level of arginase expression was low and therefore, the animals remained nitrogen vulnerable.[7] However, these murine studies were able to determine that long-term survival[36] with normal behavior and learning[37] was possible and that only low levels of hepatic arginase activity, as low as 3.5–5%, were necessary to prevent brain injury and/or death from hyperammonemia or hyperargininemia.[7] Here, we developed a CRISPR/Cas9-based strategy to deliver a codon-optimized version of human arginase 1 into hiPSCs derived from patients with arginase deficiency. *Arg1* was introduced into Exon 1 of the HPRT locus via a construct containing right and left homologous arms, the human elongation factor 1α promoter, a polyadenylation signal, and puromycin for selection (LEAPR), resulting in substantial arginase enzymatic activity in hiPSCs and in differentiated derivatives.

Cellular HPRT is an enzyme that catalyzes the conversion of hypoxanthine to inosine monophosphate and guanine to guanosine monophosphate in the nonessential purine salvage pathway.[38] Homozygous loss of HPRT function results in Lesch-Nyhan syndrome, which causes an overproduction of uric acid. However, in normal conditions, purine salvage and HPRT do not play a major role in cell growth and proliferation[39]; in therapeutic administration of cells where HPRT is not functional in the large mass of HPRT-positive cells (such as the liver), it is believed that this loss will be inconsequential in purine metabolism. There are certainly desirable selective advantages of utilizing HPRT for integrated cell selection: HPRT-positive cells are sensitive to 6-thioguanine (6-TG), killing cells by postreplicative mismatch repair[40]; additionally, this mechanism allows for secondary selection with 6-TG after HPRT locus disruption.[41,42] As transfection efficiency of hiPSCs is inherently low, the incorporation of a dual selection method with puromycin and 6-TG allowed us to purify a population of hiPSCs that contained the integrated construct at the targeted site utilizing nucleofection to deliver CRISPR/Cas9 nickases and the LEAPR cassette. In culture, these corrected hiPSCs showed that they maintained proper morphology and pluripotency, and sequencing data and qRT-PCR-based genomic integration quantification confirmed that the constructs integrated into the correct targeted site in a single HPRT allele with no off-target insertions and deletions at high unrelated probable sites. While the data demonstrate that a single X chromosome of each AD line is integrated with the donor construct, we did detect genetic mutations in the other allele of HPRT at the site of nuclease A and B activity.

Importantly, arginase was highly expressed in LEAPR-corrected cells as shown by both qRT-PCR and in urea production from functional arginase activity. After directed differentiation of LEAPR-corrected hiPSCs to the hepatic lineage, the hepatocyte-like cells were positive for albumin and α-fetoprotein, stored glycogen, and expressed multiple liver-specific RNAs. To determine if differentiation affected expression and functionality of arginase in the hepatocyte-like cells, we quantified RNA levels and urea production for comparison with their hiPSC counterparts. While RNA levels of LEAPR-derived arginase in hepatocyte-like cells were lower when compared with their hiPSC counterparts, functional arginase expression with urea production for all LEAPR-corrected hepatocyte-like cells remained, and at levels that were previously determined (with adeno-associated virus-based gene therapy) to be necessary for arginase-deficient mice to survive and be without neurodevelopmental abnormalities. As previous studies by others have shown a decline in transgene expression during differentiation with the use of the hEF1α promoter in embryonic stem cells,[43] this in part may explain the decline in expression in the hepatocyte derivatives in this study. Additionally, comparison of wild type mutated arginase and CPS1, another urea cycle enzyme, demonstrated that LEAPR modification does not negatively affect the expression of endogenous promoters of urea cycle enzymes. In aggregate, however, these data demonstrate that genetic modification at the HPRT locus of the arginase-deficient lines had no deleterious effect on their pluripotent capability and overall "stemness"; were not altered by nucleofection, selection, or culture of the hiPSCs; and were able to be differentiated into hepatocytes with restoration of arginase activity and ureagenesis.

Based on these data, integration of *Arg1* via the LEAPR expression construct by targeting the HPRT locus demonstrates the potential for restoring enzymatic activity in cells derived from hyperargininemic patients. Previously, we have shown in a murine model that with relatively low overall hepatic arginase activity establishing ureagenesis at 3.5–5% of normal led to long-term survival with controlled plasma arginine and ammonia; however these animals remained nitrogen vulnerable due to the low level of arginase expression.[7] LEAPR-corrected hepatocyte-like cells across all three lines demonstrated functionality of at least 40% compared with fetal liver; while the hEF1α promoter-based expression did decline with cellular differentiation, arginase expression in our studies remains well above the minimum threshold needed for survival and adequate nitrogen metabolism determined from the prior murine arginase studies.[7] While our present LEAPR construct contains a copy of the selection marker puromycin, an aminonucleoside antibiotic, before clinical applicability alteration of our donor construct to avoid integration of an antimicrobial resistance gene and its potential immunogenicity would be required. This would be accomplished by altering our donor construct by adding flanking *lox*P sites to the puromycin cDNA such that it could excised at the hiPSC stage prior to differentiation to the hepatocyte lineage.

Over the last 30 years, multiple studies in rodents have shown that adult hepatocyte transplantation can reverse liver failure and can correct various metabolic deficiencies of the liver.[44,45] While clinical trials of hepatocyte transplantation have demonstrated the long-term safety of cellular administration, only partial correction of metabolic disorders in humans has ever been achieved.[46,47] In part due to the limited availability of fresh donor hepatocytes of adequate quality, clinical trials, however, have been hampered and reports have been limited in general to case reports involving a few patients at most and generally with no untreated controls.[48–51] While attaining adequate engraftment will need further attention to make such therapies successful for patients with metabolic liver disorders, issues of cellular rejection should be greatly reduced[45] with an hiPSC approach as described herein.

In choosing this approach where cell availability and numbers of hepatocytes will not be a limitation, there are other important implications for treating more common monogenic disorders of the liver. The safe harbor of exon 1 of HPRT could be used in that the efficiency of homologous recombination has been demonstrated here as well as the exogenous gene expression at this locus based on the hEF1α promoter. Targeted therapy of other liver-based disorders would be easily addressed by substitution of the arginase cDNA from the donor construct with one of the other enzyme cDNA sequences from another metabolic disorder.

This study presents an approach that can be utilized to integrate an optimized cassette into a universal site distant from proto-oncogenes in patient-specific hiPSCs to restore function of abnormal liver enzymes. While we have addressed the restoration and maintenance of transgene expression pre- and postdifferentiation, additional studies are required to investigate the *in vivo* therapeutic efficacy of the corrected derivatives to maintain recovered arginase activity after cellular transplantation. Successful *in vivo* recovery of enzyme function by means of these strategies could benefit enzyme deficiencies of the urea cycle and other inborn errors of metabolism.

Materials and methods

In vitro derivation and culture of primary human dermal cells. The control human dermal fibroblast cell line (xc-HUF1), obtained from UCLA Good Manufacturing Practice (GMP) facility,[22] and two disease fibroblast lines (AD2 and AD3) used in this study were obtained from adult skin punch biopsy (after IRB approval and informed consent) and were cultured in methods previously published.[11,20] One adult disease fibroblast line (GM00954, renamed AD1) was obtained from Coriell Institute for Medical Research (Camden, NJ). All procedures were approved by the Institutional Review Board (IRB #13-001469-AM-00002) and the Embryonic Stem Cell Research Oversight (ESCRO) (ESCRO #2010-010-04A) Committee of the University of California, Los Angeles and informed consent was documented from both patients.

All fibroblast lines were cultured in media consisting of Dulbecco's modified Eagle medium nutrient mixture/F-12 (DMEM/F-12) (Invitrogen, Grand Island, NY), 10% fetal bovine serum (FBS) (Invitrogen), 1× Glutamax (Invitrogen), 1× minimum essential medium nonessential amino acid (Invitrogen) and 1× Primocin (InvivoGen, San Diego, CA). Cells were maintained in a 37°C 5% CO_2 incubator. Media was changed every 1–2 days and cells were passaged with 0.05% trypsin-ethylenediamine tetraacetic acid (EDTA) (Gemini Bio-Products, West Sacramento, CA).

In vitro derivation and culture of human stem cell lines. The control hiPSC line xc-HUF1 and the three disease hiPSC lines (AD1, AD2, and AD3) were developed by reprogramming from corresponding parental fibroblast lines via a lentiviral transduction of a stem cell cassette (STEMCCA) containing the reprogramming factors Oct4, Sox2, Klf4, and c-Myc.[52]

Fibroblasts were seeded at a confluency of 10,000 cells/cm^2 prior to transfection. After viral transduction, cells were maintained in a 37°C 5% CO_2 incubator for 3 days in a defined media consisting of DMEM/F-12 (Invitrogen) supplemented with 20% Knockout Serum Replacement (Invitrogen), 1× Glutamax (Invitrogen), 1× Minimal Essential Media NonEssential Amino Acids Solution (Invitrogen), 1× Primocin (InvivoGen), 1× β-mercaptoethanol (Millipore, Billerica, MA), and 10 µg/ml basic fibroblast growth factor (bFGF) (Biopioneer, San Diego, CA). After 3 days, the cells were passaged with 0.05% trypsin EDTA (Gemini Bio-Products) onto a layer of mouse embryonic fibroblasts (GlobalStem, Rockville, MD) and maintained in culture up to 30 days until putative hiPSC colonies began to form.

All cells were transitioned to and subsequently maintained in feeder-free culture conditions consisting of reduced growth factor Matrigel (BD Biosciences, San Jose, CA) and a 50:50 mix of mTeSR1 media (StemCell Technologies, Vancouver, BC, Canada) and Nutristem (Stemgent, San Diego, CA) supplemented with 1× Primocin (InvivoGen) and 10 µg/ml bFGF. Cells were mechanically passaged every 4 to 5 days, depending on confluency and colony size. To passage the cells, pulled glass pipettes were used to cross-hatch the colonies and to lift the pieces gently for transfer onto new Matrigel-coated plates.

DNA delivery by nucleofection. Cells were prepared for nucleofection by aspirating the media from each well and replacing with 2 ml of mTeSR/Nutristem media supplemented with 10 µmol/l ROCK inhibitor (BioPioneer, San Diego, CA). After 1 hour, the media was again aspirated and replaced with 1 ml Stempro Accutase (Life Technologies, Carlsbad, CA) and incubated at 37ºC for 4–6 minutes in 1–2 ml of mTeSR1/Nutristem media supplemented with 10 µmol/l ROCK inhibitor in each well to neutralize the Accutase. Cells were then washed and gently scraped into suspension. The cell suspension was transferred to a sterile 15 ml conical tube and centrifuged for 5 minutes at 80*g*. The supernatant was aspirated and the cells were resuspended in an appropriate volume of mTeSR1/Nutristem media with ROCK inhibitor. 10 µl of the resuspended sample was removed and counted by hemocytometer. Samples planned for nucleofection were prepared as 800,000–1 million cells each. Aliquots were centrifuged for 5 minutes at 80*g*. Supernatant were aspirated and the cells were resuspended in 100 µl of nucleofection solution (Lonza, Walkersville, MD) and placed into nucleofection cuvettes. (Care was taken to carefully resuspend cells to maximize the amount of single cells in suspension and to minimize cell death due to excessive mechanical stress). 1–2 µg of each DNA vector was added and mixed into the nucleofection solution. Controls, 1–2 µg of pMAX-GFP, which is included in the kit, were added to one aliquot of each cell solution. The samples were then securely placed into an Amaxa Nucleofector II (Lonza) and nucleofected using the B-016 program to facilitate cellular DNA vector uptake. The cells were then pipetted into either previously prepared Matrigel-coated plates or directly onto previously prepared plates of mouse embryonic fibroblasts. 72 hours after plating, mTeSR1/Nutristem media was supplemented with 1 µg/ml of puromycin for an additional 72 hours. Following puromycin selection, cells were cultured in mTeSR1/Nutristem media without puromycin. Colonies were expanded until large enough to isolate by mechanical passaging.

Hepatocyte differentiation of iPSCs. To begin hepatocyte differentiation, hiPSCs were passaged at 90% confluency. The next day, the differentiation protocol began as previously published.[17] Briefly, hiPSCs were incubated for 24 hours with Roswell Park Memorial Institute (RPMI) 1640 medium (Life Technologies, Carlsbad, CA), and supplemented with 0.5 mg/ml bovine serum albumin (BSA; Sigma-Aldrich, St. Louis, MO), 100 ng/ml Recombinant Human Activin A (Peprotech, Rocky Hill, NJ), and 1× Primocin (Invivogen). On days 2 and 3, 0.1% and 1% insulin-transferrin-selenium (Life Technologies) were added to the previous supplemented RPMI 1640 medium, respectively. On day 4, hiPSCs were cultured with Hepatocyte Culture Medium (HCM) (consisting of HBM Basal Medium and HCM SingleQuot Kit) (Lonza) supplemented with 30 ng/ml Recombinant Human Fibroblast Growth Factor-4 (FGF-4) (Peprotech), 20 ng/ml Bone Morphogenetic Protein-2 (BMP-2) (Peprotech), and 1× Primocin (Invivogen) for 4 days. The differentiated cells were then cultured in HCM containing 20 ng/ml Recombinant Human Hepatocyte Growth Factor (HGF), 20 ng/ml Recombinant Human Keratinocyte Growth Factor (KGF), and 1× Primocin (Invivogen) for 6 days, and then in HCM supplemented with 10 ng/ml Recombinant Human Oncostatin M (OSM) (R&D Systems, Minneapolis, MN), 0.1 µmol/l dexamethasone (Sigma), and 1× Primocin (Invivogen) for the following 5 days. For the last 3 days of the hepatic differentiation, the cells were cultured in DMEM/F:12 (Life Technologies) supplemented with 1× N2, 1× B27, 1× GlutaMAX (Life Technologies), 1× NEAA (Life Technologies), 0.1 mmol/l β-mercaptoethanol (Life Technologies), and 1× Primocin (Invivogen). All media and supplements were filtered prior to use with a 0.22 micron filter and media was changed daily.

Immunocytochemistry. Cells were washed with phosphate buffered saline (PBS) and fixed with 4% paraformaldehyde (Polysciences, Warrington, PA) in 1× PBS for 15 minutes prior to staining. When necessary, samples were permeabilized in 1% Triton X-100 (Sigma-Aldrich, St. Louis, MO) in PBS for 1 hour at room temperature. Subsequently, all samples were blocked with 5% goat serum (Sigma) in PBS for 1 hour at room temperature. Primary antibodies were diluted to working concentrations in 5% goat serum; cells were incubated with the primary antibody overnight in 4°C. After incubation, cells were washed three times with PBS at 5 minutes per wash. Secondary antibodies were diluted in 5% goat serum and cells were incubated for 1 hour at RT. Cells were washed three times with PBS and incubated with 1×4,6-diamidino-2-2-phenylindole (DAPI; Thermo, Waltham, MA) for 7 minutes. Fluorescence images were captured with an Axiocam MR Monocolor Camera and AxioVision Digital Image Processing Software (Axio Observer Inverted Microscope; Carl Zeiss, Jena, Germany). The primary and secondary antibodies used for hiPSC and hepatocyte-like cells are listed in **Table 1**.

Teratoma formation and analysis. Teratomas for the control and disease hiPSC lines were generated by injecting 1×10^6 cells (resuspended in Matrigel (BD Biosciences)) subcutaneously into both hind limbs of male severe combined immunodeficient (SCID) mice (Charles River Laboratories, San Diego, CA). Tumors were harvested roughly 1–1.5 months after injection and fixed in 4% paraformaldehyde. Tissues were routinely processed and paraffin-embedded followed by staining with hematoxylin and eosin (H&E). All animal experiments adhered to policies set by the UCLA Animal Research Committee and the UCLA Division of Laboratory Animal Medicine (Protocol #2006-119-22).

Karyotype analysis. The hiPSCs were cultured to 95–99% confluency in 25 cm^2 flasks and delivered to Cell Line Genetics (Madison, WI) for G-band karyotyping analysis.

Reverse transcription PCR. RNA was extracted from primary fibroblasts, hiPSCs, and hepatocyte-like cells with a Roche High Pure RNA Isolation Kit (Roche Applied Sciences, Indianapolis, IN) and 10 ng–1 µg was reversed transcribed to cDNA with the Transcriptor First Strand cDNA synthesis kit (Roche Applied Sciences) following the manufacturer's instructions. Primers were designed in NCBI/Primer-Blast and synthesized by Valugene (San Diego, CA) and are listed in **Table 2**. RT-PCR was performed with 25 ng of cDNA from each sample and each reaction was prepared with 12.5 µl 2× KAPA Fast Genotyping Mix (Kapa Biosystems, Wilmington, MA) and with 10 µmol/l forward and reverse primers and was run on a LightCycler 480 Real-Time PCR System (Roche Applied Sciences). Gels were made with 2% agarose (Bio-Rad Laboratories, Hercules, CA) and 1× SYBR Safe DNA Gel Stain (Life Technologies) in tris-acetate-EDTA (TAE) buffer and run on a PowerPac Basic Power Supply (Bio-Rad) at 90 V for 30 minutes.

Table 1 Primary and secondary antibodies used to demonstrate pluripotency and to characterize hepatocyte-like cells

	Primary antibody		Secondary antibody		
	Reference	Dilution	Isotype	Reference	Dilution
Oct-3/4	SCBT, Santa Cruz, CA, SC-5279	1:100	Donkey anti-Rabbit IgG Alexa Fluor 546	Life Technologies, Carlsbad, CA, A-10036	1:250
Nanog	Abcam, Cambridge, MA, ab80892	1:100	Goat anti-Rabbit IgG (H+L) Alexa Fluor 488	Life Technologies, A-11008	1:500
SSEA-3	Millipore, mab4303	1:200	Goat anti-Rat IgM Alexa Fluor 594	Life Technologies, A-21213	1:500
SSEA-4	Millipore, mab4304	1:200	Goat anti-Mouse IgG (H+L) Alexa Fluor 488	Life Technologies, A-11001	1:500
TRA-1–60	Millipore, mab4360	1:200	Goat anti-Mouse IgM Alexa Fluor 488	Life Technologies, A-20142	1:500
TRA-1–81	Millipore, mab4381	1:200	Goat anti-Mouse IgM Alexa Fluor 488	Life Technologies, A-20142	1:500
Albumin	R&D Systems, Minneapolis, MN mab1455	1:50	Goat anti-Mouse IgG (H+L) Alexa Fluor 488	Life Technologies, A-11001	1:250
Alpha-fetoprotein	Life Technologies, 18-0003	1:50	Goat anti-Mouse IgG (H+L) Alexa Fluor 488	Life Technologies, A-11001	1:250

Table 2 List of reverse transcription-polymerase chain reaction (RT-PCR) forward (F) and reverse (R) primer sets for hepatic markers

Gene	Primer sequence	Amplicon
AAT	F: 5′ AAGGACACCGAGGAAGAGGA 3′ R: 5′ CACCCCTGAAGCTCTCCAAG 3′	393
ALB	F: 5′ ACCCCAAGTGTCAACTCCAA 3′ R: 5′ CTGAAAAGCATGGTCGCCTG 3′	224
CK18	F: 5′ ACACAGTCTGCTGAGGTTGG 3′ R: 5′ GCCTCCAGCTTGACCTTGAT 3′	275
CPS1	F: 5′ TTTAGGGCAATGGCTACAGG 3′ R: 5′ GTTCTGCAAGAGCTGGGTTC 3′	541
CYP3A4	F: 5′ GGTGGTGAATGAAACGCTCAG 3′ R: 5′ ACACACCCTTTGGAAGTGGACC 3′	243
FIX	F: 5′ TGGAGATCAGTGTGAGTCCAAT 3′ R: 5 'ACATGGAAATGGCACTGCTGG 3′	256
GAPDH	F: 5′ TGAAGGTCGGACTCAACGGATTTGGT 3′ R: 5′ CATGTGGGCCATGAGGTCCACCAC 3′	983
TDO2	F: 5′ TGGAGACGATGACAGCCTTG 3′ R: 5′ AGCAGGAAAAGACACTTCTGGA 3′	214
TF	F: 5′ ATTACGTCAACAGCAGCACCT 3′ R: 5′ GCTGTAGGGAAAGACCAGACG 3′	533
UDP-GT	F: 5′ GTGTCCCATGCTGGGAAGAT 3′ R: 5′ CTGACGGACCCTTTCCTTCC 3′	394

AAT, alpha 1-antitrypsin; *ALB*, human serum albumin; *CK18*, cytokeratin 18; *CPS1*, carbamoyl phosphate synthase 1; *CYP3A4*, cytochrome p450 3A4; *FIX*, factor IX, *GAPDH*, glyceraldehyde 3-phosphate dehydrogenase; *TF*, transferrin; *TDO2*, tryptophan 2,3-dioxygenase; *UDP-GT*, uridine diphosphate glucuronyltransferase.

Quantitative RT-PCR. Total RNA was isolated from cultures with a Roche High Pure RNA Isolation Kit (Roche Applied Sciences) and 250 ng–1 µg was reverse transcribed to cDNA utilizing a Transcriptor First Strand cDNA Synthesis Kit (Roche Applied Sciences). Primers for endogenous arginase and human codon-optimized arginase and probes (designed from the Roche Universal Probe Library) were synthetized at Valuegene (**Table 3**). Quantitative PCR relative gene expression experiments were performed with 10 ng of cDNA on a LightCycler 480 Real-Time PCR System (Roche) and data was analyzed with LightCycler 480 Software (release 1.5.0.). Triplicate experimental samples were paired using the all-to-mean pairing rule ΔCt value calculation with GAPDH for advanced relative quantification.

Cloning and gene optimization. pUC18-HPRTx1-LHA-hEF1α-ArgO-IRES-PAC-HPRTx1-RHA was cloned by PCR of HPRTx1 (Exon 1)-RHA(*R*ight *H*omologous *A*rm) with primers 5′-HPRT-RHA-NotI (GCATGCGGCCGCCAGTCAGCCCGC-GCGCC) and 3′-HPRT-RHA-PstI (CGATCTGCAGCCTGC-CGCCCTCGCGT) and restriction enzyme digested with NotI and PstI. HPRTx1-LHA (*L*eft-*H*omologous-*A*rm) was synthesized by GeneWiz, removed and isolated from pUC57-Kan by digestion with EcoRI and XbaI. hEF1α-ArgO-IRES-PAC was removed and isolated from pRRL-hEF1α-ArgO-IRES-PAC with XbaI+NotI digest. Two synthetic polyadenylation sequences[53] were inserted 3′ of HPRTx1-LHA and 5′ of HPRTx1-RHA by cutting and inserting the sequences with SpeI and NotI, respectively. Oligonucleotides were synthesized by ValueGene and annealed together to create inserts for cloning. Finally, all inserts were ligated together with pUC18 digested by EcoRI and PstI. DNA was introduced into cells by nucleofection (see Supplementary Experimental Procedures for details).

Table 3 List of reverse transcription-quantitative polymerase chain reaction (RT-qPCR) forward (F) and reverse (R) primer sets for wild type Arginase 1 (*Arg1*) and the human codon optimized arginase (*ArgO*), carbamoyl-phosphate synthetase 1 (CPS1), and glyceraldehyde 3-phosphate dehydrogenase (GAPDH)

Gene	Primer sequence	Amplicon	Probe
ARG1 WT	F: 5′ CAGGATTAGATATAATGGAAGTGAACC 3′ R: 5′ CTGCTGTGTTCACTGTTCGAG 3′	78	60
ArgO	F: 5′ AAGGTGATGGAGGAGACATTG 3′ R: 5′ CGTCAACATCGAAGGACAGA 3′	76	69
CPS1	F: 5′ CAAGTTTTGCAGTGGAATCG 3′; R: 5′ ACGGATCATCACTGGGTAGC 3′	74	74
GAPDH	F: 5′ GCTCTCTGCTCCTCCTGTTC 3′; R: 5′ ACGACCAAATCCGTTGACTC 3′	115	60

Human codon optimized arginase (*ArgO*) was developed by running the amino acid sequence of *Arg1* through Gene Designer 2.0 software (DNA2.0, Menlo Park, CA) against the *homo sapiens* codon usage table. Once the initial sequence was produced, it was run through NetGene2 (http://www.cbs.dtu.dk/services/NetGene2/) to find any cryptic splice sites. This sequence was then checked for any long repeats in Oligonucleotides Repeat Finder (http://wwwmgs.bionet.nsc.ru/mgs/programs/oligorep/InpForm.htm). Any variations needed to delete splice sites or long repeats were silent mutations that used the next most common codon in the *Homo sapiens* codon usage table.

Junction PCR and sequencing analysis. To verify targeted integration of our donor vector in corrected hiPSCs, each 5′ and 3′ junction of the integrated vector was analyzed by PCR and DNA sequencing. Reactions were prepared with genomic DNA, 12.5 µl of Phusion High-Fidelity PCR Master Mix (New England BioLabs, Ipwich, MA), 10.25 µl of water, and 1.25 µl of forward and reverse primers for the 3′ and 5′ ends of Exon 1 of HPRT (**Table 4**).

For sequencing, PCR bands were extracted and purified using the Wizard SV Gel and PCR Cleanup System (Promega, Madison WI) and the purified products were sent to Laragen (Culver City, CA) for sequencing analysis.

Off target analysis. To identify potential introduced mutations at other regions in the genome, off-target binding/cutting of the DNA by the CRISPR/Cas9 nucleases resulting in insertions or deletions was analyzed at the predicted most common sites for each CRISPR/cas9 nickase as determined by the MIT CRISPR Design website (http://www.crispr.mit.edu). Each corresponding gDNA region sequence was downloaded from the PubMed genebank. PCR primers were designed using the ThermoFisher primer designer (http://www.thermofisher.com/oligoperfect.html). Appropriate primers were synthesized by Integrated DNA Technologies (Coralville, IA) to amplify each off-target region. For particularly GC-rich regions, 5% dimethylsulfoxide (DMSO) or Betaine (Sigma) was added. The region on the other HPRT allele was amplified using the same 5′F and 3′R junction PCR primers as was used for junction PCR analysis. Each potential off-target region was amplified by PCR from both the parental and genetically modified gDNA samples of AD1

Table 4 List of reverse transcription-polymerase chain reaction (RT-PCR) forward (F) and reverse (R) primer sets for the 3′ and 5′ junctions of Exon 1 of the hypoxanthine-guanine phosphoribosyltransferase (*HPRT*) gene

Gene	*Primer sequence*
HPRT 5′	F: 5′ CCTGATCTGGGTGACTCTAGGACT 3′ R: 5′ CACGACATCACTTTCCCAGTTTAC 3′
HPRT 3′	F: 5′ TGCAAGAACTCTTCCTCACG 3′ R: 5′ GCATCTCCATAAAGATGAACTACAGTGTGCAAAAC 3′

Table 5 List of reverse transcription-quantitative polymerase chain reaction (RT-qPCR)-based genomic integration analysis forward (F) and reverse (R) primer sets for genomic hypoxanthine-guanine phosphoribosyltransferase (gHPRT) and genomic glyceraldehyde 3-phosphate dehydrogenase (gGAPDH)

Gene	Primer sequence	Amplicon	Probe
gHPRT	F: 5′ CGGTAGAGGAGAGGGTAGAGC 3′ R: 5′ ACAGGACTGGCAAAGGTGAG 3′	62	65
gGAPDH	F: 5′ GCCTCAAGATCATCAGGTGAG 3′ R: 5′ CAGGGGAGCGTGTCCATA 3′	76	64

using the Phusion PCR Master Mix (ThermoFisher). PCR conditions were set according to manufacturer recommendations: (i) 98°C 30 seconds, (ii) 98°C 10 seconds, (iii) 57°C 30 seconds, (iv) 72°C 1 minute, Repeat 2–4 35×, (v) 72°C 5 minutes, and (vi) 4°C hold using Phusion high-fidelity PCR master mix (ThermoFisher). PCR products were run on a 1% agarose gel for ~20 minutes at 100 V. Bands were extracted using the Wizard SV Gel and PCR Cleanup System, followed manufacturer protocol and were sequenced by Laragen.

To also determine if both HPRT alleles were integrated with the LEAPR construct, we performed quantitative real time PCR (*ArgO*, gGAPDH, and gHPRT) of each AD line knowing that AD1 and AD3 were XX and AD2 was XY (**Table 5**). Knowing this, we reasoned that we should see twice as much gHPRT in AD1 and AD3 compared with AD2 (**Supplementary Figure S2**, top). In addition, we reasoned that we should see the same amount of *ArgO* expression in all three AD lines relative to GAPDH (**Supplementary Figure S2**, middle). Finally, if only one allele was integrated we should detect half as much *ArgO* expression in AD1 and AD3 compared with AD2, relative to HPRT (*i.e.*, 1 copy of *ArgO* per two copies of HPRT in AD1 and AD3 compared with 1 copy of *ArgO* per one copy of HPRT in AD2) (**Supplementary Figure S2**, bottom).

Functional assay for arginase activity. Arginase activity was measured in cell lysates. 2×10^6–4×10^6 cells were pelleted by low-speed centrifugation and frozen for each sample. Cell pellets were lysed at 20,000 cells/µl in lysis buffer. Primary tissue sample controls were homogenized with 40 µl of lysis buffer/mg of tissue. Lysis buffer was prepared with 0.1% Triton X-100 and 1× HALT protease inhibitor cocktail (Thermo) and urea production was measured as previously performed.[36,54] Briefly, samples were centrifuged at 100*g* for 5 minutes at 4°C and the supernatant was collected. An activated mixture, consisting of 12.5 µl of 50 mmol/l Tris-Cl (pH 7.5), 12.5 µl of 10 mmol/l MnCl, and 25 µl of the supernatant was incubated at 56°C for 10 minutes. 2.5 µl of the activated mixture was added to 25 µl of 0.5 mol/l arginine (pH 9.7) and incubated at 37°C for 1 hour. After incubation, 72.5 µl ddH_2O was added to bring the final volume to 100 µl. 400 µl of an acid mixture, consisting of one part H_2SO_4 (95%), three parts H_3PO_4 (85%), and seven parts ddH_2O, in addition to 25 µl of 9% isonitrosopropiophenone (ISPF) in ethanol, was added to samples and urea standards. Urea standards were prepared at 9.3, 18.7, 37.5, 75, 150, and 300 µg/ml in ddH_2O. The final mixture was incubated at 100°C for 45 minutes. After incubation, samples were cooled to room temperature and protected from light for 10 minutes. 200 µl of each sample was aliquoted in duplicate and measured at an optical density of 540 nm in a 96-well plate in a plate reader (Bio-Rad).

Sequencing analysis. Fibroblasts were cultured in 25 cm^2 flasks and delivered to GeneDx (Gaithersberg, MD) for complete *Arg1* gene sequencing and mutation analysis. Mutations were analyzed in hiPSC and hepatocyte progeny in the UCLA Orphan Disease lab by PCR followed by Sanger sequencing. Select regions of the *Arg1* gene were amplified by PCR using standard conditions (95° for 2 minutes (1 cycle)); 94° for 30 seconds, 60° for 30 seconds, 72° for 1 minute (35 cycles); 72° for 3 minutes (1 cycle); hold at 10°). Primer sequences for the c.61C>T variant were as follows: (5′-TTTGCACAAACTACTTG TTCACTG-3′; 5′-TCAGAGTGGGGAGGAAATCA-3′). Primers for the c.365G>A variant were as follows: (5′-AAAACCAA GTGGGAGCATTG-3′; 5′-CCTTCCACCTCCTGAATGTC-3′). Primers for the c.709G>A variant were as follows: (5′-CATG AAATAATGGGTTGCTACTTTT-3′; 5′-TTGCTTCTCTATTACC TCAGATTGTT-3′). Primers for the c.892G>C variant were as follows: (5′-CCATCGGTTACTACCTTTTTCTG-3′; 5′-TCTG AAAGAACAAGTCTTTAGAAGG-3′). An aliquot of each PCR product was confirmed by gel electrophoresis based on its predicted amplicon size. The rest of the PCR product was purified using the QIAquick PCR purification kit (Qiagen) and subjected to bidirectional sequencing using ABI BigDye v3.1 terminators on an ABI 3130xl genetic analyzer (Applied Biosystems, Foster City, CA). The sequence traces at each location were manually analyzed for the presence of a variant using the SequenceScanner v.1 software (Applied Biosystems) in comparison to the GenBank reference sequence NM_000045.3.

Statistical analysis. All collected data was analyzed with the SPSS (Armonk, NY) statistical package (Version 21.0). Results were expressed as mean ± standard deviation (SD) and *P*-values were determined using a one-way analysis of variance (ANOVA) to examine significance across comparisons. Error bars represent SD.

Supplementary material

Figure S1. Integration of LEAPR cassette in AD2 and AD3 hiPSCs.
Figure S2. Determining single integration of LEAPR into HPRT locus in corrected hiPSCs.
Figure S3a. Off target analysis of nickase A for potential insertions or deletions.
Figure S3b. Off target analysis of nickase B for potential insertions or deletions.
Figure S4. Measuring ArgO in AD2 and AD3 hiPSCs.
Figure S5. Measuring ArgO in AD2 and AD3 hepatocyte-like cells.

Figure S6a. Characterization of AD2 and AD3 hepatocyte-like cells.

Figure S6b. Characterization of AD2 and AD3 hepatocyte-like cells.

Figure S7. Measuring Wild-type Arg1 and CPS1 levels in uncorrected and corrected hiPSCs and hepatocytes.

Acknowledgments P.C.L. derived all disease hiPSC lines, performed characterization studies on hiPSC lines optimized differentiation of hiPSCs into hepatocyte-like cells, differentiated hiPSCs into hepatocyte-like cells, performed characterization studies of hepatocyte-like cells, compiled data, and wrote the manuscript. B.T. aided in disease hiPSC line generation, optimized differentiation of hiPSCs into hepatocyte-like cells, differentiated hiPSCs into hepatocyte-like cells, performed characterization studies of hepatocyte-like cells, performed quantitative real-time PCR and urea functional analyses on hiPSCs and hepatocyte-like cells, performed mouse studies, compiled data, and wrote the manuscript. A.V.C. aided in disease hiPSC line generation and the design and consultation of experiments, grew fibroblasts, and performed mouse studies. W.B.G., K.H., and S.K. designed the human codon optimized arginase and LEAPR constructs and also performed integration experiments on hiPSCs. S.K., J.K.T., K.M.C., A.L., and B.S. aided in the differentiation, characterization, and cloning experiments. J.B. helped conceive some of the experiments. G.S.L. conceived the experiments, oversaw the experiments, analyzed the data, and wrote the manuscript. All authors contributed to the preparation of the experiments, results, and drafting of the manuscript. This research was supported by the grant CIRM TR4-06831 from the California Institute of Regenerative Medicine (to G.S.L.). The authors thank Haolei Wan (UCLA) for performing the sequencing and mutation analysis of the AD progeny lines. The authors declare no conflict of interest.

1. Summar, ML, Koelker, S, Freedenberg, D, Le Mons, C, Haberle, J, Lee, HS, *et al.* (2013). The incidence of urea cycle disorders. *Mol Genet Metab* **110**: 179–180.
2. Deignan, JL, Cederbaum, SD and Grody, WW (2008). Contrasting features of urea cycle disorders in human patients and knockout mouse models. *Mol Genet Metab* **93**: 7–14.
3. Uchino, T, Snyderman, SE, Lambert, M, Qureshi, IA, Shapira, SK, Sansaricq, C *et al.* (1995). Molecular basis of phenotypic variation in patients with argininemia. *Hum Genet* **96**: 255–260.
4. Foschi, FG, Morelli, MC, Savini, S, Dall'Aglio, AC, Lanzi, A, Cescon, M *et al.* (2015). Urea cycle disorders: a case report of a successful treatment with liver transplant and a literature review. *World J Gastroenterol* **21**: 4063–4068.
5. Ah Mew, N, Lanpher, BC, Gropman, A, Chapman, KA, Simpson, KL *et al.* (1993). *Urea cycle disorders overview.* In: Pagon RA *et al.* (eds.). *Gene Reviews(R),* Seattle (WA) https://www.ncbi.nlm.nih.gov/books/NBK1116.
6. Cederbaum, SD, Yu, H, Grody, WW, Kern, RM, Yoo, P and Iyer, RK (2004). Arginases I and II: do their functions overlap? *Mol Genet Metab* **81 (Suppl 1)**: S38–S44.
7. Hu, C, Tai, DS, Park, H, Cantero, G, Cantero-Nieto, G, Chan, E *et al.* (2015). Minimal ureagenesis is necessary for survival in the murine model of hyperargininemia treated by AAV-based gene therapy. *Gene Ther* **22**: 111–115.
8. Jain-Ghai, S, Nagamani, SC, Blaser, S, Siriwardena, K and Feigenbaum, A (2011). Arginase I deficiency: severe infantile presentation with hyperammonemia: more common than reported? *Mol Genet Metab* **104**: 107–111.
9. Kasten, J, Hu, C, Bhargava, R, Park, H, Tai, D, Byrne, JA *et al.* (2013). Lethal phenotype in conditional late-onset arginase 1 deficiency in the mouse. *Mol Genet Metab* **110**: 222–230.
10. Luiking, YC, Engelen, MP and Deutz, NE (2010). Regulation of nitric oxide production in health and disease. *Curr Opin Clin Nutr Metab Care* **13**: 97–104.
11. Byrne, JA, Nguyen, HN and Reijo Pera, RA (2009). Enhanced generation of induced pluripotent stem cells from a subpopulation of human fibroblasts. *PLoS One* **4**: e7118.
12. Lowry, WE, Richter, L, Yachechko, R, Pyle, AD, Tchieu, J, Sridharan, R *et al.* (2008). Generation of human induced pluripotent stem cells from dermal fibroblasts. *Proc Natl Acad Sci USA* **105**: 2883–2888.
13. Takahashi, K and Yamanaka, S (2006). Induction of pluripotent stem cells from mouse embryonic and adult fibroblast cultures by defined factors. *Cell* **126**: 663–676.
14. Takahashi, K, Tanabe, K, Ohnuki, M, Narita, M, Ichisaka, T, Tomoda, K *et al.* (2007). Induction of pluripotent stem cells from adult human fibroblasts by defined factors. *Cell* **131**: 861–872.
15. Yu, J, Vodyanik, MA, Smuga-Otto, K, Antosiewicz-Bourget, J, Frane, JL, Tian, S *et al.* (2007). Induced pluripotent stem cell lines derived from human somatic cells. *Science* **318**: 1917–1920.
16. Chen, YF, Tseng, CY, Wang, HW, Kuo, HC, Yang, VW and Lee, OK (2012). Rapid generation of mature hepatocyte-like cells from human induced pluripotent stem cells by an efficient three-step protocol. *Hepatology* **55**: 1193–1203.
17. Song, Z, Cai, J, Liu, Y, Zhao, D, Yong, J, Duo, S *et al.* (2009). Efficient generation of hepatocyte-like cells from human induced pluripotent stem cells. *Cell Res* **19**: 1233–1242.
18. Zhang, Z, Huang, B, Gao, F and Zhang, R (2015). Impact of immune response on the use of iPSCs in disease modeling. *Curr Stem Cell Res Ther* **10**: 236–244.
19. Jinek, M, Chylinski, K, Fonfara, I, Hauer, M, Doudna, JA and Charpentier, E (2012). A programmable dual-RNA-guided DNA endonuclease in adaptive bacterial immunity. *Science* **337**: 816–821.
20. Durruthy-Durruthy, J, Briggs, SF, Awe, J, Ramathal, CY, Karumbayaram, S, Lee, PC *et al.* (2014). Rapid and efficient conversion of integration-free human induced pluripotent stem cells to GMP-grade culture conditions. *PLoS One* **9**: e94231.
21. Somers, A, Jean, JC, Sommer, CA, Omari, A, Ford, CC, Mills, JA *et al.* (2010). Generation of transgene-free lung disease-specific human induced pluripotent stem cells using a single excisable lentiviral stem cell cassette. *Stem Cells* **28**: 1728–1740.
22. Karumbayaram, S, Lee, P, Azghadi, SF, Cooper, AR, Patterson, M, Kohn, DB *et al.* (2012). From skin biopsy to neurons through a pluripotent intermediate under good manufacturing practice protocols. *Stem Cells Transl Med* **1**: 36–43.
23. Baxter, M, Withey, S, Harrison, S, Segeritz, CP, Zhang, F, Atkinson-Dell, R *et al.* (2015). Phenotypic and functional analyses show stem cell-derived hepatocyte-like cells better mimic fetal rather than adult hepatocytes. *J Hepatol* **62**: 581–589.
24. Gau, CL, Rosenblatt, RA, Cerullo, V, Lay, FD, Dow, AC, Livesay, J *et al.* (2009). Short-term correction of arginase deficiency in a neonatal murine model with a helper-dependent adenoviral vector. *Mol Ther* **17**: 1155–1163.
25. Strulovici, Y, Leopold, PL, O'Connor, TP, Pergolizzi, RG and Crystal, RG (2007). Human embryonic stem cells and gene therapy. *Mol Ther* **15**: 850–866.
26. Meyburg, J and Hoffmann, GF (2010). Liver, liver cell and stem cell transplantation for the treatment of urea cycle defects. *Mol Genet Metab* **100 (Suppl 1)**: S77–S83.
27. Bachmann, C (2003). Outcome and survival of 88 patients with urea cycle disorders: a retrospective evaluation. *Eur J Pediatr* **162**: 410–416.
28. Enns, GM, Berry, SA, Berry, GT, Rhead, WJ, Brusilow, SW and Hamosh, A (2007). Survival after treatment with phenylacetate and benzoate for urea-cycle disorders. *N Engl J Med* **356**: 2282–2292.
29. Schambach, A, Cantz, T, Baum, C and Cathomen, T (2010). Generation and genetic modification of induced pluripotent stem cells. *Expert Opin Biol Ther* **10**: 1089–1103.
30. Liu, H, Kim, Y, Sharkis, S, Marchionni, L and Jang, YY (2011). *In vivo* liver regeneration potential of human induced pluripotent stem cells from diverse origins. *Sci Transl Med* **3**: 82ra39.
31. Gerecht-Nir, S and Itskovitz-Eldor, J (2004). Human embryonic stem cells: a potential source for cellular therapy. *Am J Transplant* **4 (Suppl 6)**: 51–57.
32. Giudice, A and Trounson, A (2008). Genetic modification of human embryonic stem cells for derivation of target cells. *Cell Stem Cell* **2**: 422–433.
33. Yusa, K, Rashid, ST, Strick-Marchand, H, Varela, I, Liu, PQ, Paschon, DE *et al.* (2011). Targeted gene correction of α1-antitrypsin deficiency in induced pluripotent stem cells. *Nature* **478**: 391–394.
34. Musunuru, K (2013). Genome editing of human pluripotent stem cells to generate human cellular disease models. *Dis Model Mech* **6**: 896–904.
35. Young, CS, Hicks, MR, Ermolova, NV, Nakano, H, Jan, M, Younesi, S *et al.* (2016). A single CRISPR-Cas9 deletion strategy that targets the majority of DMD patients restores dystrophin function in hiPSC-derived muscle cells. *Cell Stem Cell* **18**: 533–540.
36. Lee, EK, Hu, C, Bhargava, R, Rozengurt, N, Stout, D, Grody, WW *et al.* (2012). Long-term survival of the juvenile lethal arginase-deficient mouse with AAV gene therapy. *Mol Ther* **20**: 1844–1851.
37. Lee, EK, Hu, C, Bhargava, R, Ponnusamy, R, Park, H, Novicoff, S *et al.* (2013). AAV-based gene therapy prevents neuropathology and results in normal cognitive development in the hyperargininemic mouse. *Gene Ther* **20**: 785–796.
38. Silverman, LJ, Kelley, WN and Palella, TD (1987). Genetic analysis of human hypoxanthine-guanine phosphoribosyltransferase deficiency. *Enzyme* **38**: 36–44.
39. Liao, S, Tammaro, M and Yan, H (2015). Enriching CRISPR-Cas9 targeted cells by co-targeting the HPRT gene. *Nucleic Acids Res* **43**: e134.
40. Swann, PF, Waters, TR, Moulton, DC, Xu, YZ, Zheng, Q, Edwards, M *et al.* (1996). Role of postreplicative DNA mismatch repair in the cytotoxic action of thioguanine. *Science* **273**: 1109–1111.
41. Shaw-White, JR, Denko, N, Albers, L, Doetschman, TC and Stringer, JR (1993). Expression of the lacZ gene targeted to the HPRT locus in embryonic stem cells and their derivatives. *Transgenic Res* **2**: 1–13.

42. Narsinh, KH and Wu, JC (2010). Gene correction in human embryonic and induced pluripotent stem cells: promises and challenges ahead. *Mol Ther* **18**: 1061–1063.
43. Hong, S, Hwang, DY, Yoon, S, Isacson, O, Ramezani, A, Hawley, RG *et al.* (2007). Functional analysis of various promoters in lentiviral vectors at different stages of *in vitro* differentiation of mouse embryonic stem cells. *Mol Ther* **15**: 1630–1639.
44. Soltys, KA, Soto-Gutiérrez, A, Nagaya, M, Baskin, KM, Deutsch, M, Ito, R *et al.* (2010). Barriers to the successful treatment of liver disease by hepatocyte transplantation. *J Hepatol* **53**: 769–774.
45. Bhatia, SN, Underhill, GH, Zaret, KS and Fox, IJ (2014). Cell and tissue engineering for liver disease. *Sci Transl Med* **6**: 245sr2.
46. Fox, IJ, Chowdhury, JR, Kaufman, SS, Goertzen, TC, Chowdhury, NR, Warkentin, PI *et al.* (1998). Treatment of the Crigler-Najjar syndrome type I with hepatocyte transplantation. *N Engl J Med* **338**: 1422–1426.
47. Puppi, J, Tan, N, Mitry, RR, Hughes, RD, Lehec, S, Mieli-Vergani, G *et al.* (2008). Hepatocyte transplantation followed by auxiliary liver transplantation–a novel treatment for ornithine transcarbamylase deficiency. *Am J Transplant* **8**: 452–457.
48. Dhawan, A, Mitry, RR, Hughes, RD, Lehec, S, Terry, C, Bansal, S *et al.* (2004). Hepatocyte transplantation for inherited factor VII deficiency. *Transplantation* **78**: 1812–1814.
49. Horslen, SP, McCowan, TC, Goertzen, TC, Warkentin, PI, Cai, HB, Strom, SC *et al.* (2003). Isolated hepatocyte transplantation in an infant with a severe urea cycle disorder. *Pediatrics* **111**(6 Pt 1): 1262–1267.
50. Muraca, M, Gerunda, G, Neri, D, Vilei, MT, Granato, A, Feltracco, P *et al.* (2002). Hepatocyte transplantation as a treatment for glycogen storage disease type 1a. *Lancet* **359**: 317–318.
51. Sokal, EM, Smets, F, Bourgois, A, Van Maldergem, L, Buts, JP, Reding, R *et al.* (2003). Hepatocyte transplantation in a 4-year-old girl with peroxisomal biogenesis disease: technique, safety, and metabolic follow-up. *Transplantation* **76**: 735–738.
52. Sommer, CA, Stadtfeld, M, Murphy, GJ, Hochedlinger, K, Kotton, DN and Mostoslavsky, G (2009). Induced pluripotent stem cell generation using a single lentiviral stem cell cassette. *Stem Cells* **27**: 543–549.
53. Levitt, N, Briggs, D, Gil, A and Proudfoot, NJ (1989). Definition of an efficient synthetic poly(A) site. *Genes Dev* **3**: 1019–1025.
54. Hu, C, Kasten, J, Park, H, Bhargava, R, Tai, DS, Grody, WW *et al.* (2014). Myocyte-mediated arginase expression controls hyperargininemia but not hyperammonemia in arginase-deficient mice. *Mol Ther* **22**: 1792–1802.

Supplementary Information accompanies this paper on the Molecular Therapy–Nucleic Acids website (http://www.nature.com/mtna)